N-body Simulations with generic non-Gaussian Initial Conditions

Paper I: arXiv:1006.5793 (JCAP 2010)
Paper II: arXiv:1102.3229

Christian Wagner

with Licia Verde and Lotfi Boubekeur

20 April 2011, Avignon

Outline

- Introduction
- Initial Condition Generation
- Simulations
- Results
- Conclusions

Primordial Non-Gaussianity

- Inflation generates an almost Gaussian random field
- Statistically described by the power spectrum (2-point): $P(k)=Ak^{n-4}$
- Nearly Gaussian PDF of the perturbations (1-point)
- Skewness $\langle\Phi^3\rangle \neq 0$

  => non-zero bispectrum $B(k_1,k_2,k_3)$ (3-point)
- Non-vanishing higher-order statistics (n-point)

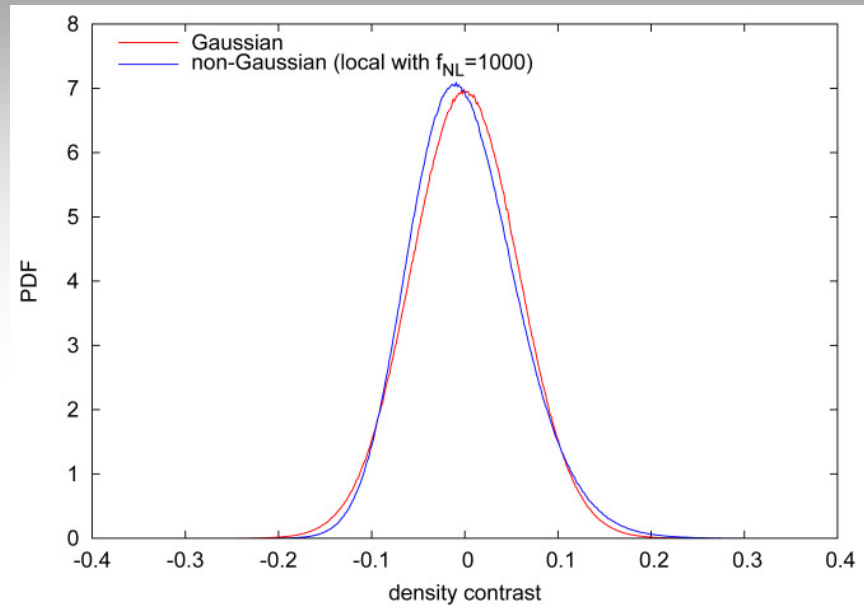

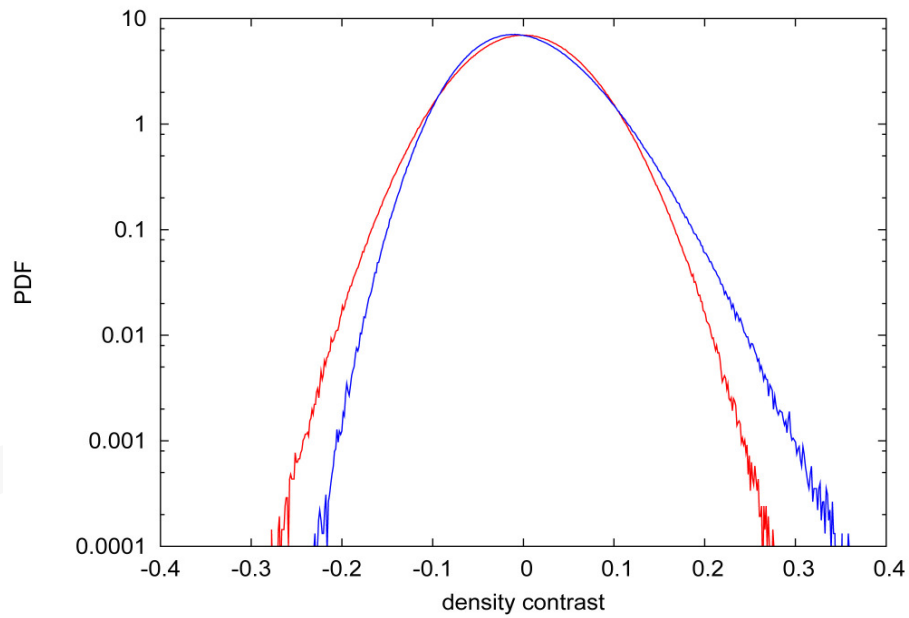

Different inflationary models generate different bispectrum shapes

$$\langle \Phi_{k_1} \Phi_{k_2} \Phi_{k_3} \rangle = (2\pi)^3 \delta^D(\mathbf{k}_1 + \mathbf{k}_2 + \mathbf{k}_3) B(k_1, k_2, k_3)$$

Triangle configuration for which the bispectrum peaks

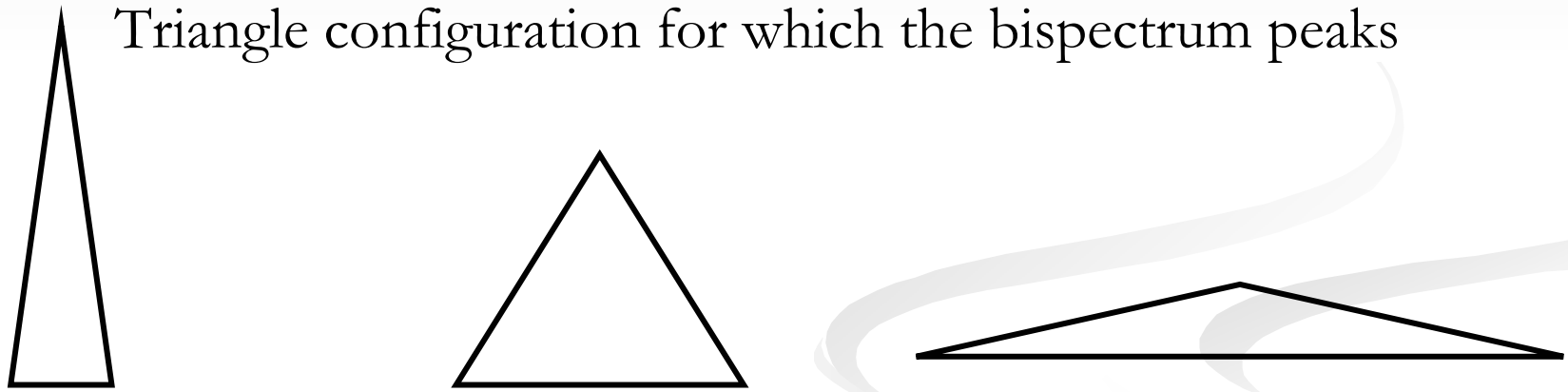

Squeezed / local **equilateral** **flattened /enfolded**

orthogonal (to the equilateral and local shape)

Probes of non-Gaussianity

- **Cosmic Microwave Background**

$$-10 < f_{NL}^{\rm local} < 74$$
$$-214 < f_{NL}^{\rm equil} < 266$$
$$-410 < f_{NL}^{\rm orthog} < 6$$

(Komatsu et al. 2010)

- **Large-scale structure**:
  - Abundance of very rare objects: galaxy clusters (or voids)

    Local: $f_{NL} = 449 \pm 286$ (Cayon et al. 2010, see also Hoyle et al. 2010 and Enqvist et al. 2010, however Mortonson et al. 2010)

  - Scale-dependent halo bias on large scales

    Local: $-27 < f_{NL} < 70$ (Slosar et al. 2008, see also Xia et al. 2010)

  - Halo bispectrum

    e.g. Nishimichi et al 2009 (simulations) and Baldauf et al. 2010 (PT)

Non-Gaussian halo mass function

- Press-Schechter for non-Gaussian fields
- Two different approximations:
  - MVJ (Matarrese, Verde, Jimenez 2000)
  - LoVerde et al. 2008
- Skewness is the relevant parameter
- For other analytic approaches see next talk talk (De Simone et al. 2007, Ma et al. 2007, D'Amico et al. 2010)

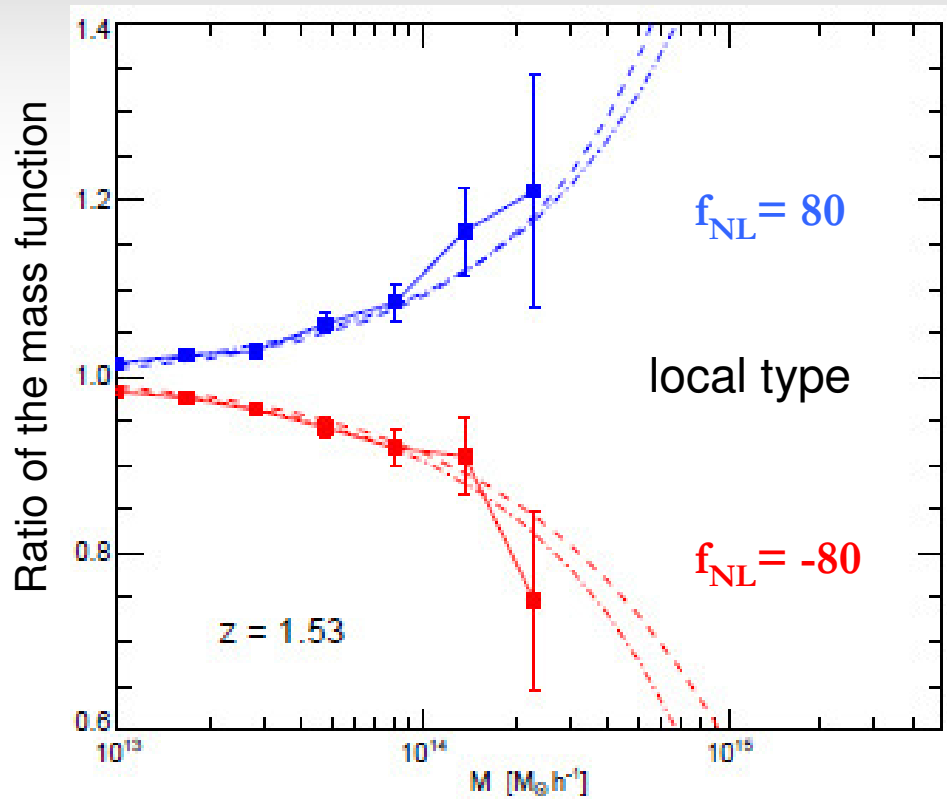

Grossi et al. 2009

Non-Gaussian halo bias

- Scale-dependent halo bias on large scales (Dalal et al. 2008)
- High peak approach (Matarrese and Verde 2009)
- Peak Background Split (Slosar et al. 2008, Schmidt et al. 2010)

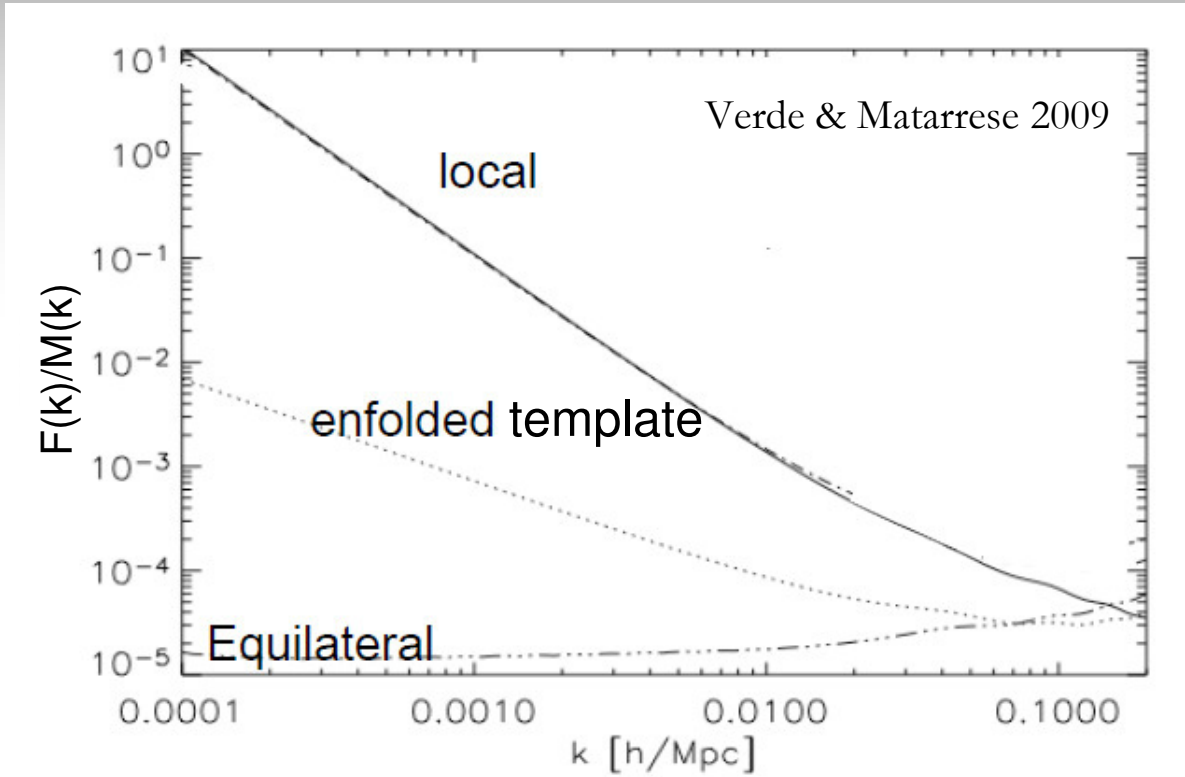

$$b^{\rm NG}_{M,z}(k, f_{\rm NL}) = b_{1;M,z}(f_{\rm NL}) + f_{\rm NL}\left[b_{1;M,z}(f_{\rm NL}) - 1\right]\frac{q\delta_c}{D(z)}\frac{\mathcal{F}_M(k)}{\mathcal{M}_M(k)} + \text{non-linear corrections}$$

Non-Gaussian halo bias

- Scale-dependent halo bias on large scales (Dalal et al. 2008)
- High peak approach (Matarrese and Verde 2009)
- Peak Background Split (Slosar et al. 2008, Schmidt et al. 2010)

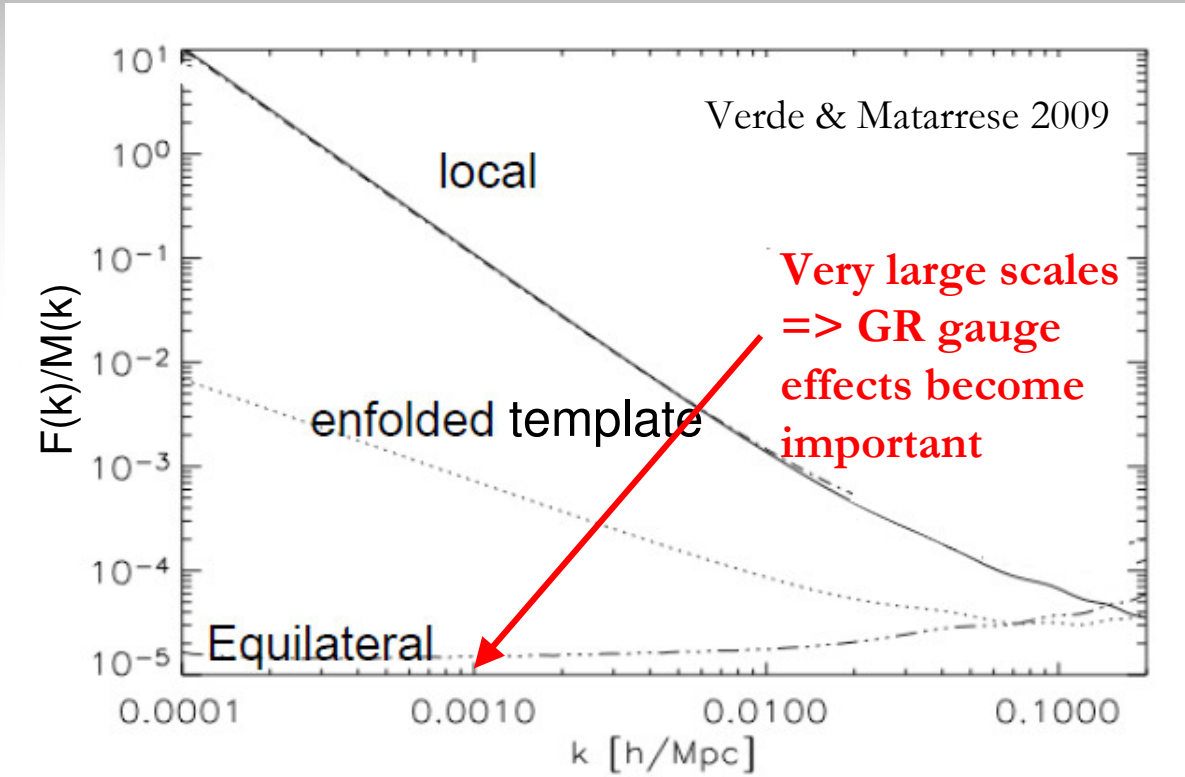

$$b^{\rm NG}_{M,z}(k, f_{\rm NL}) = b_{1;M,z}(f_{\rm NL}) + f_{\rm NL}\left[b_{1;M,z}(f_{\rm NL}) - 1\right]\frac{q\delta_c}{D(z)}\frac{\mathcal{F}_M(k)}{\mathcal{M}_M(k)} + \text{non-linear corrections}$$

Non-Gaussian halo bias

- Scale-dependent halo bias on large scales (Dalal et al. 2008)
- High peak approach (Matarrese and Verde 2009)
- Peak Background Split (Slosar et al. 2008, Schmidt et al. 2010)

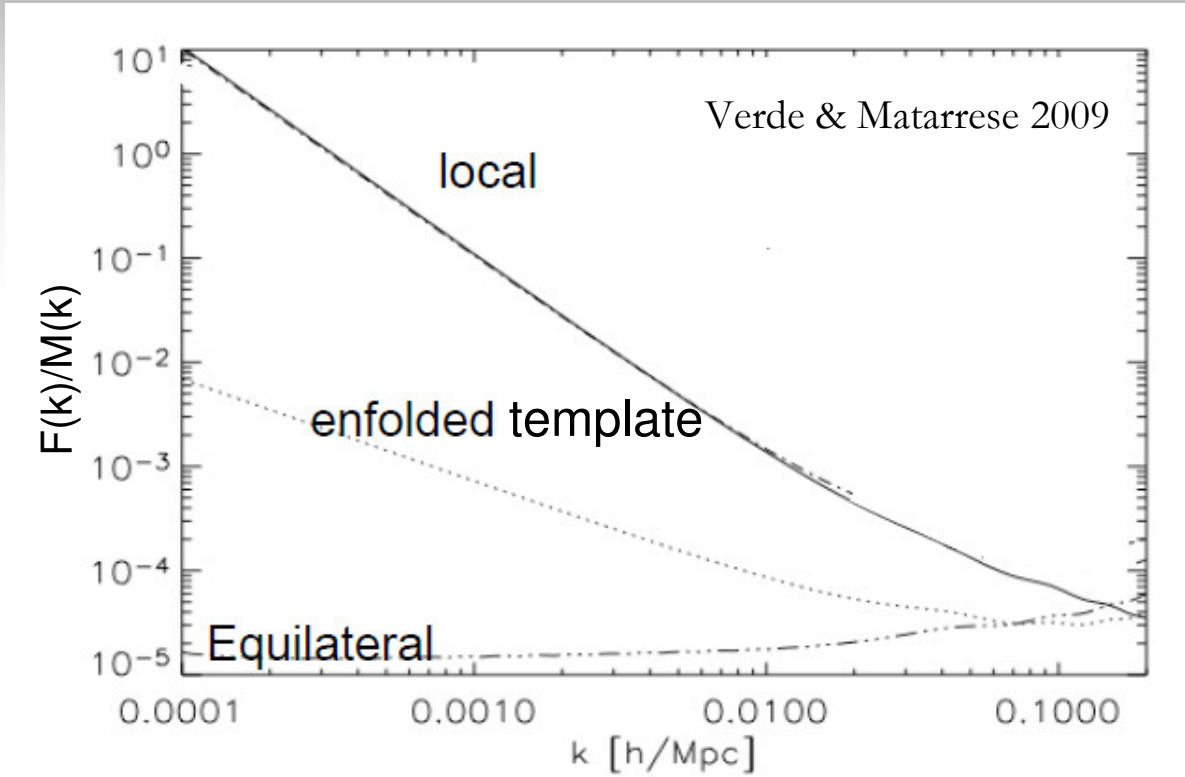

$$b^{\rm NG}_{M,z}(k, f_{\rm NL}) = b_{1;M,z}(f_{\rm NL}) + f_{\rm NL}\,[b_{1;M,z}(f_{\rm NL}) - 1]\,\frac{q\delta_c}{D(z)}\frac{\mathcal{F}_M(k)}{\mathcal{M}_M(k)} + \text{non-linear corrections}$$

Linear bias

$$b_1 = 1 - \frac{\partial \ln n(M,z)}{\partial \delta_c}$$

Non-Gaussian halo bias

- Scale-dependent halo bias on large scales (Dalal et al. 2008)
- High peak approach (Matarrese and Verde 2009)
- Peak Background Split (Slosar et al. 2008, Schmidt et al. 2010)

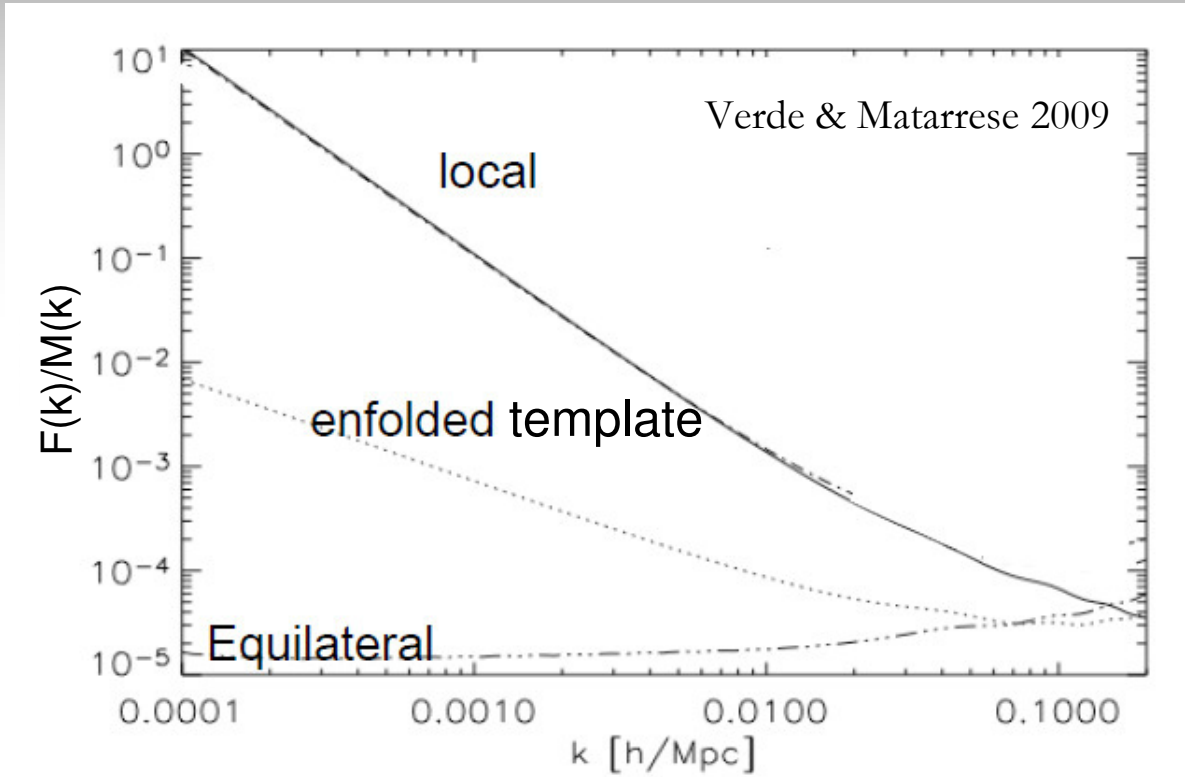

$$b^{\rm NG}_{M,z}(k, f_{\rm NL}) = b_{1;M,z}(f_{\rm NL}) + f_{\rm NL}\left[b_{1;M,z}(f_{\rm NL}) - 1\right]\frac{q\delta_c}{D(z)}\frac{\mathcal{F}_M(k)}{\mathcal{M}_M(k)} + \text{non-linear corrections}$$

Linear bias

$$b_1 = 1 - \frac{\partial \ln n(M,z)}{\partial \delta_c}$$

Collapse threshold with fudge factor q

Non-Gaussian halo bias

- Scale-dependent halo bias on large scales (Dalal et al. 2008)
- High peak approach (Matarrese and Verde 2009)
- Peak Background Split (Slosar et al. 2008, Schmidt et al. 2010)

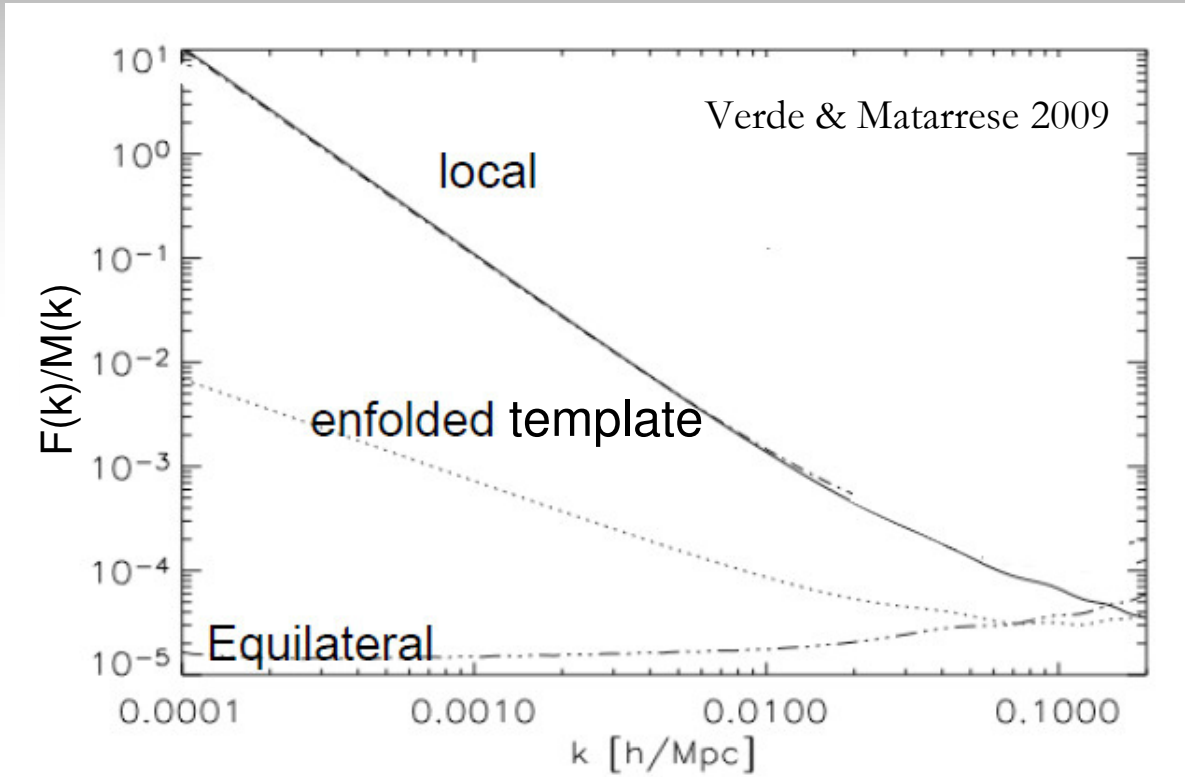

$$b^{\rm NG}_{M,z}(k, f_{\rm NL}) = b_{1;M,z}(f_{\rm NL}) + f_{\rm NL}\left[b_{1;M,z}(f_{\rm NL}) - 1\right]\frac{q\delta_c}{D(z)}\frac{\mathcal{F}_M(k)}{\mathcal{M}_M(k)} + \text{non-linear corrections}$$

Linear bias

$$b_1 = 1 - \frac{\partial \ln n(M,z)}{\partial \delta_c}$$

Collapse threshold with fudge factor q

Poisson Equation and CMB physics

$$\frac{2}{3}\frac{T(k)k^2}{\Omega_m H_0^2}W_M(k)$$

Non-Gaussian halo bias

- Scale-dependent halo bias on large scales (Dalal et al. 2008)
- High peak approach (Matarrese and Verde 2009)
- Peak Background Split (Slosar et al. 2008, Schmidt et al. 2010)

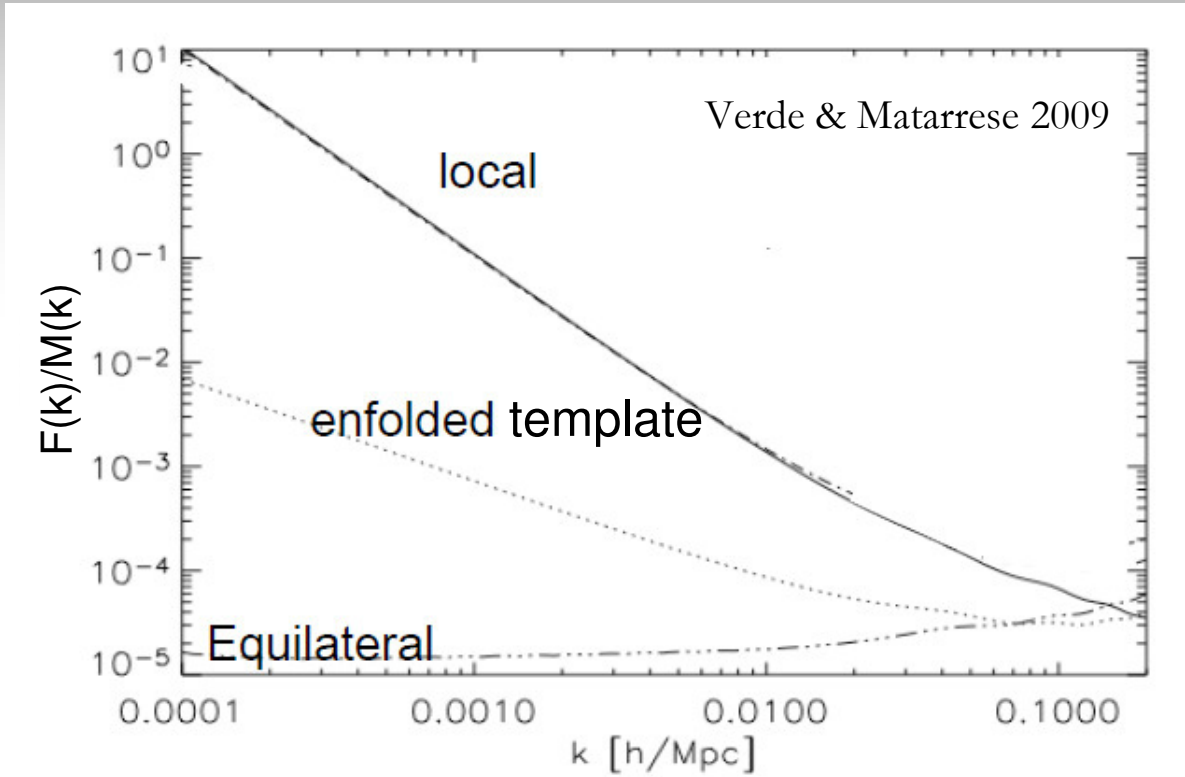

$$b^{\rm NG}_{M,z}(k, f_{\rm NL}) = b_{1;M,z}(f_{\rm NL}) + f_{\rm NL}\left[b_{1;M,z}(f_{\rm NL}) - 1\right]\frac{q\delta_c}{D(z)}\frac{\mathcal{F}_M(k)}{\mathcal{M}_M(k)} + \text{non-linear corrections}$$

Form Factor

$$\mathcal{F}_M(k) = \frac{1}{8\pi^2\sigma_M^2 f_{\rm NL}}\int dk' k'^2 \mathcal{M}_M(k')\int_{-1}^{1} d\mu \mathcal{M}_M(|\mathbf{k}+\mathbf{k}'|)\frac{B_\Phi(k,k',|\mathbf{k}+\mathbf{k}'|)}{P_\Phi(k)}$$

Templates vs. physical shapes

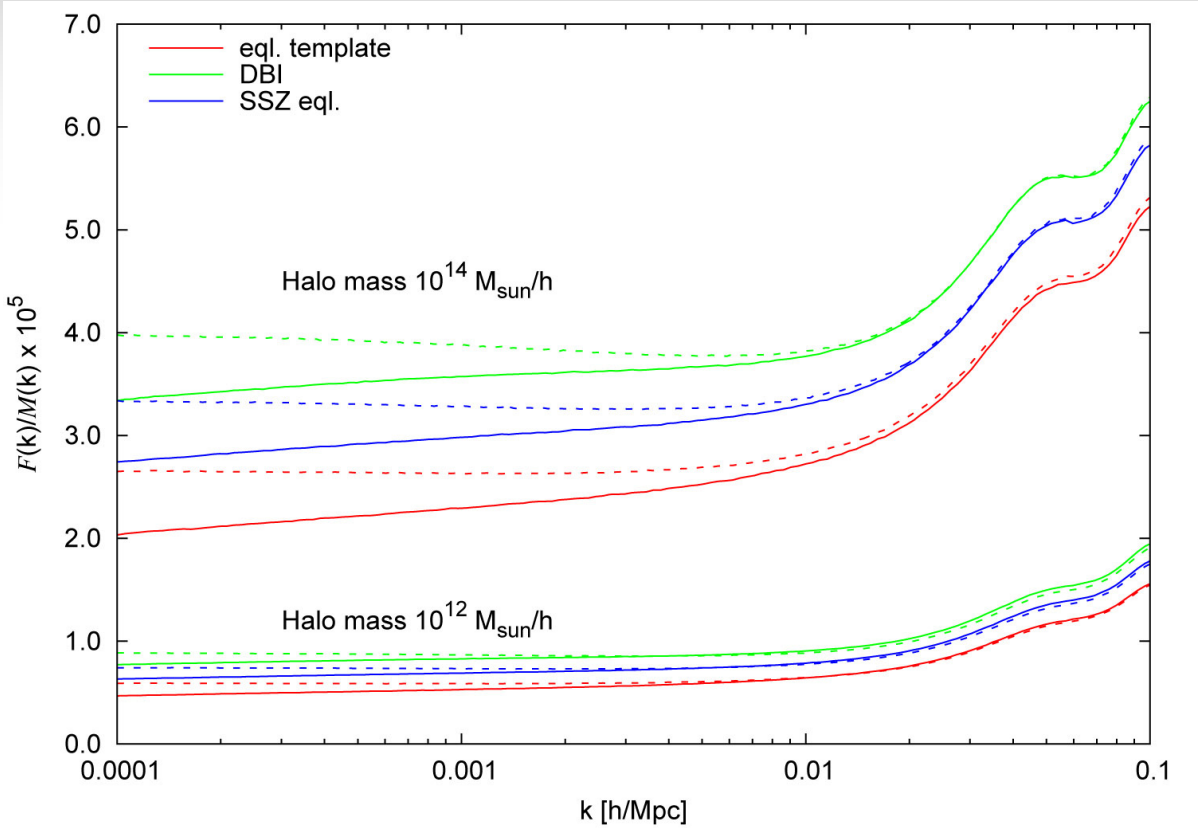

- **templates** approximate the physical bispectra over all triangle configurations and are **factorizable** => allows efficient computation

- however, for the **NG bias** the correct scaling in the **squeezed limit** is crucial

dashed lines: scale-invariant power spectrum
solid lines: spectral index n_s=0.95

Templates vs. physical shapes

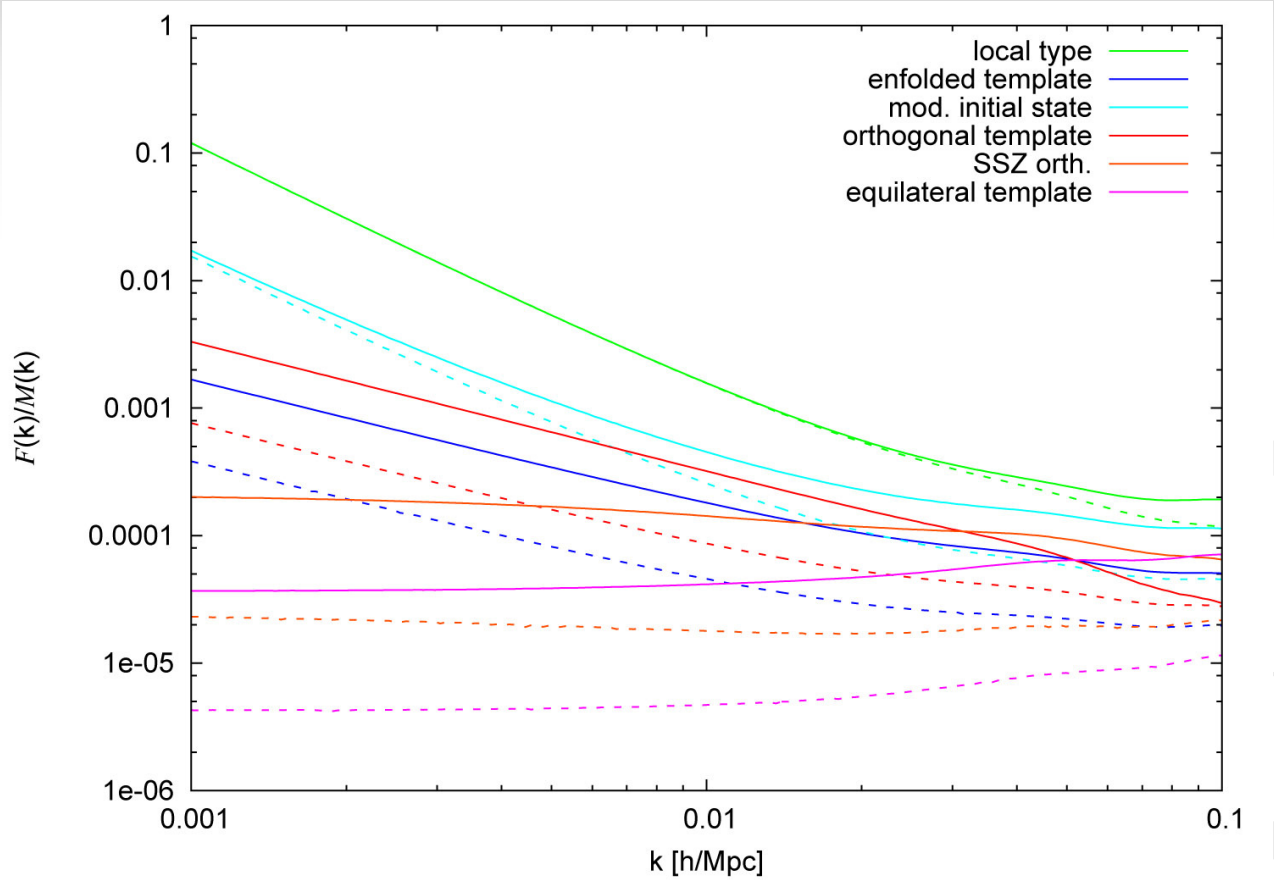

- modified initial state/enfolded template template (Meerburg et al. 2009)
- orthogonal template (Senatore et al. 2010)
- these templates do **not** have the correct scaling in the squeezed limit

solid lines: $M_{halo} \sim 10^{14}\ M_{sun}/h$ **dashed lines:** $M_{halo} \sim 10^{11}\ M_{sun}/h$

N-body Simulations

- Halo formation is a highly non-linear process => N-body simulations
- Analytic predictions have been tested with N-body simulations by many groups
- Papers:
  - Dalal et al. 2008
  - Grossi et al. 2007 and 2010
  - Desjacques et al. 2009
  - Pillepich et al. 2010
  - …

- But up to very recently **only the local type** was simulated!

Outline

- Introduction
- Initial Condition Generation
- Simulations
- Results
- Conclusions

Initial Conditions

- Split the Potential into a Gaussian and a (small) non-Gaussian part

$$\Phi_{\mathbf{k}} = \Phi_{\mathbf{k}}^{G} + \Phi_{\mathbf{k}}^{NG}$$

- Generate a Gaussian Random field

  $\Phi^{G}_{k} \sim N\{0, (P(k)/2)^{1/2}\} + i\, N\{0, (P(k)/2)^{1/2}\}$

  $P(k)=A\, k^{n-4}$ where n is the spectral index

- Poisson equation and CMB physics

$$\delta_{\mathbf{k}} = \frac{2}{3}\frac{k^2 T(k) D(z)}{\Omega_m H_0^2}\Phi_{\mathbf{k}}$$

- Use Zel'dovich Approximation or 2LPT to obtain particle positions and velocities

How to get ϕ^{NG}

- Ansatz for Φ^{NG} for a given bispectrum

  old (Paper I):

$$\Phi_{\mathbf{k}}^{NG} = \frac{1}{6(2\pi)^3}\int d^3k_2 B_\Phi(k, k_2, |\mathbf{k}+\mathbf{k}_2|)\frac{\Phi_{\mathbf{k}_2}^{*G}}{P(k_2)}\frac{\Phi_{\mathbf{k}+\mathbf{k}_2}^{G}}{P(|\mathbf{k}+\mathbf{k}_2|)}$$

  new (Paper II):

$$\Phi_{\mathbf{k}}^{NG} = \frac{1}{2(2\pi)^3}\int d^3k' \frac{B_\Phi(k, k', |\mathbf{k}+\mathbf{k}'|)\Phi_{\mathbf{k}'}^{*G}\Phi_{\mathbf{k}+\mathbf{k}'}^{G}}{P_\Phi(k)P_\Phi(k') + P_\Phi(k')P_\Phi(|\mathbf{k}+\mathbf{k}'|) + P_\Phi(k)P_\Phi(|\mathbf{k}+\mathbf{k}'|)}$$

- In both cases:

$$\langle \Phi_{k_1}^G \Phi_{k_2}^G \Phi_{k_3}^{NG}\rangle = \frac{1}{3}(2\pi)^3 B(k_1, k_2, k_3)\delta^D(\mathbf{k}_1+\mathbf{k}_2+\mathbf{k}_3)$$

- The old ansatz gives rise to spurious divergences in the power spectrum, the new ansatz does not!
- But computationally very expensive: cost ~ N_g^6

If the Bispectrum is factorizable

$$B(k_1, k_2, k_3) \equiv \sum_i b_1^i(k_1) b_2^i(k_2) b_3^i(k_3)$$

- The old ansatz can be written as a sum of convolution
- Compute convolutions with the help of Fast Fourier Transforms => very significant speed up of the IC generation

$$\Phi_{\mathbf{k}}^{NG} = \frac{1}{6} \sum_i b_1^i(k) \int \frac{d^3 k_2}{(2\pi)^3} G^i(\mathbf{k}_2) Q^i(\mathbf{k} + \mathbf{k}_2)$$

$$G^i(\mathbf{k}) = b_2^i(k) \Phi_{\mathbf{k}}^{*G} / P(k)$$

$$Q^i(\mathbf{k}) = b_3(k) \Phi_{\mathbf{k}}^{G} / P(k)$$

- Using a so-called Schwinger parameter the new ansatz can also be factorized

$$\frac{k_1^3 k_2^3 k_3^3}{k_1^3 + k_2^3 + k_3^3} = k_1^3 k_2^3 k_3^3 \int_0^\infty \mathrm{d}t \exp\left[-t\left(k_1^3 + k_2^3 + k_3^3\right)\right]$$

(see e.g. Smith & Zaldarriaga 2006)

If the Bispectrum is factorizable

$$B(k_1, k_2, k_3) \equiv \sum_i b_1^i(k_1) b_2^i(k_2) b_3^i(k_3)$$

- The old ansatz can be written as a sum of convolution
- Compute convolutions with the help of Fast Fourier Transforms => very significant speed up of the IC generation

$$\Phi_{\mathbf{k}}^{NG} = \frac{1}{6} \sum_i b_1^i(k) \int \frac{d^3 k_2}{(2\pi)^3} G^i(\mathbf{k}_2) Q^i(\mathbf{k} + \mathbf{k}_2)$$

$$G^i(\mathbf{k}) = b_2^i(k) \Phi_{\mathbf{k}}^{*G} / P(k)$$

$$Q^i(\mathbf{k}) = b_3(k) \Phi_{\mathbf{k}}^{G} / P(k)$$

- Using a so-called Schwinger parame new ansatz can als factorized

$$k_1^3 k_2^3 k_3^3 \qquad \infty \qquad \mathrm{xp}\left[-t\left(k_1^3 + k_2^3 + k_3^3\right)\right]$$

WORK IN PROGRESS

(see e.g. Smith & Zaldarriaga 2006)

Outline

- Introduction
- Initial Condition Generation
- Simulations
- Results
- Conclusions

Using a smaller grid for ϕ_k^{NG}

- Initial ϕ_k^{NG} computation scales as ~ N_g^6
- Choose a grid size for ϕ_k^{NG} of 400 (computation takes 2 days on 256 cores)
- Gaussian grid size is 1024
- Box size 1875 Mpc/h

  => "NG resolution" 5 Mpc/h ~ 3×10^{13} M_{sun}/h
- One billion particles per simulation

  => Particle mass ~ 5×10^{11} M_{sun}/h
- Evolve simulation with Gadget-2 (takes 1 day on 256 cores)
- Numerical tests confirmed the expected lower mass limit of resolved halos to be **3×10^{13} M_{sun}/h**

Simulations

Table 1. N-body simulations. N_g denotes the size of the grid used for the non-Gaussian part of the potential. The size of the particle grid is identical to the size of the grid used for the Gaussian part of the potential and is given by N_p.

type of non-Gaussianity	$f_{\rm NL}$	N_g	N_p	# realizations
local	250	400	1024	1
local	250	1024	1024	2
local	60	1024	1024	3
equilateral template	1000	400	1024	2
equilateral template[a]	1000	1024	1024	1
orthogonal template	-1000	400	1024	2
orthogonal template	-250	400	1024	3
Gaussian	-	-	1024	3

[a] In this case, we use ansatz Eq. (4.5) for the non-Gaussian $\Phi_{\mathbf{k}}^{NG}$. The convolution is computed with an FFT in real space.

Simulation data is publicly available at:

`http://icc.ub.edu/~liciaverde/NGSCP.html`

Outline

- Introduction
- Initial Condition Generation
- Simulations and Numerical Tests
- Results
- Conclusions

NG halo bias – local ~ k^{-3} (squeezed limit)

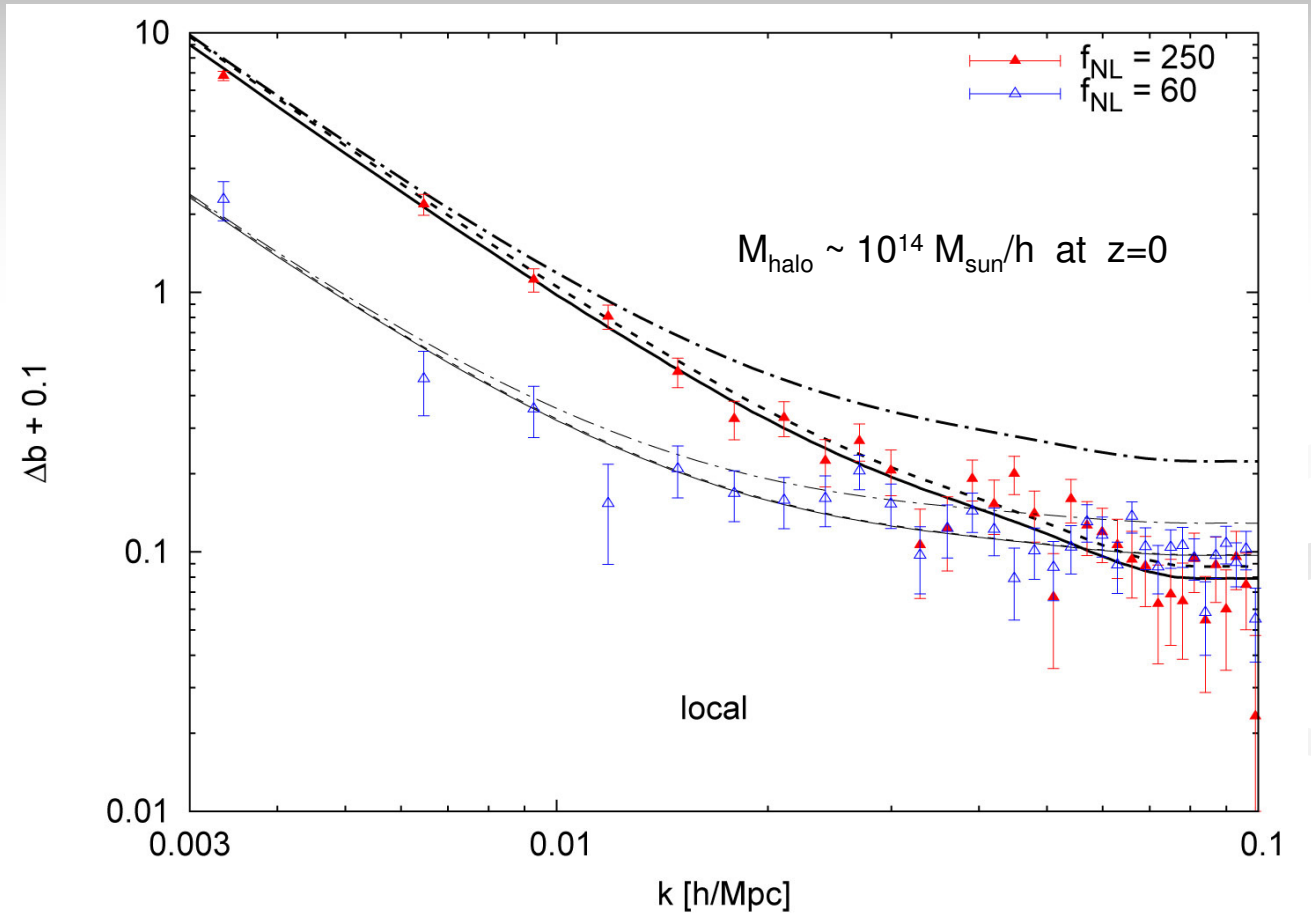

$$\Delta b(k) = \Delta b_I + f_{\rm NL}\left[b_1^G + \Delta b_I - 1\right]\frac{q\delta_c}{D(z)}\frac{\mathcal{F}_M(k)}{\mathcal{M}_M(k)}$$

NG halo bias – local ~ k^{-3} (squeezed limit)

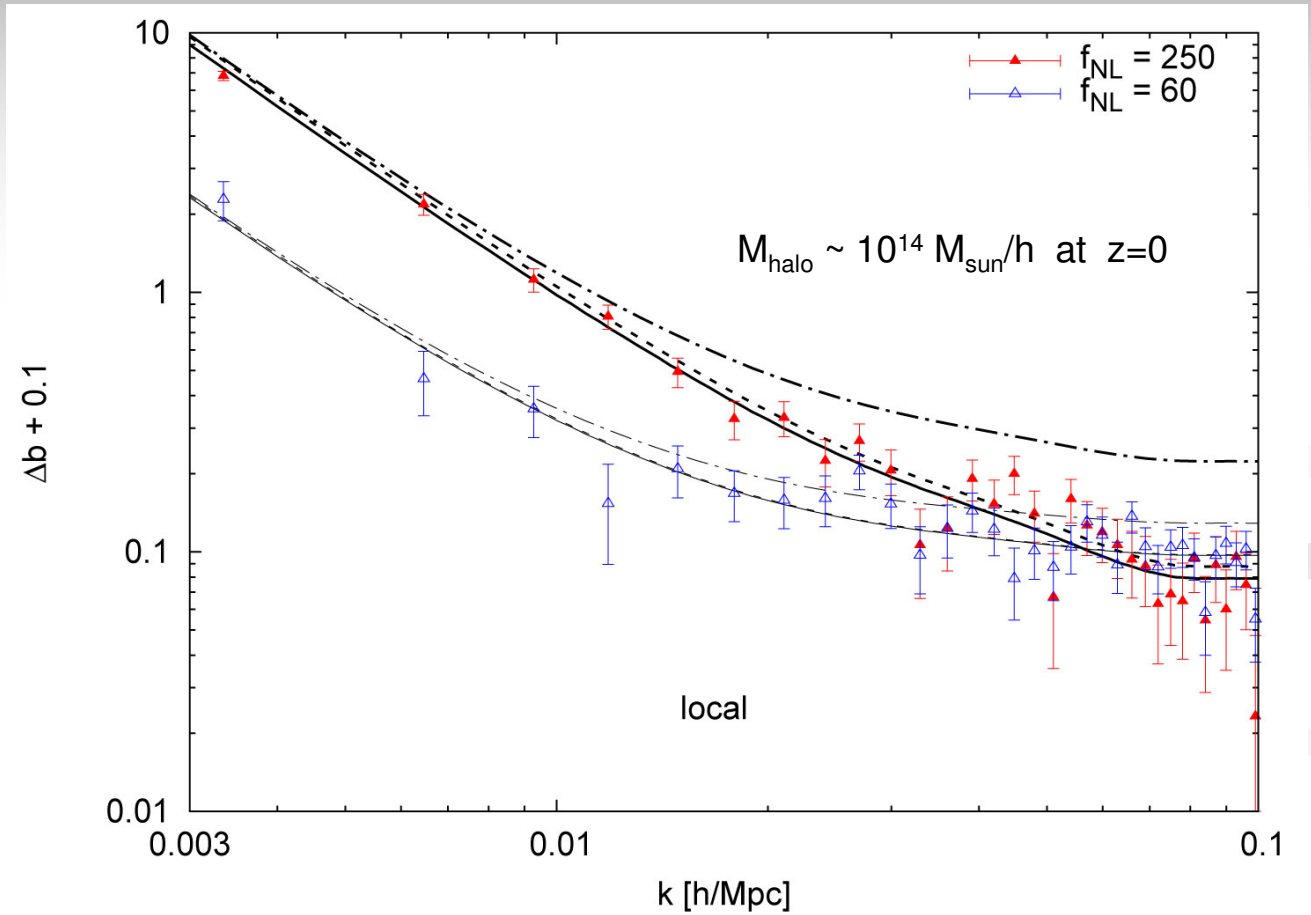

$$\Delta b(k) = \Delta b_I + f_{\rm NL}\left[b_1^G + \cancel{\Delta b_I} - 1\right]\frac{q\delta_c}{D(z)}\frac{\mathcal{F}_M(k)}{\mathcal{M}_M(k)}$$

NG halo bias – local ~ k^{-3} (squeezed limit)

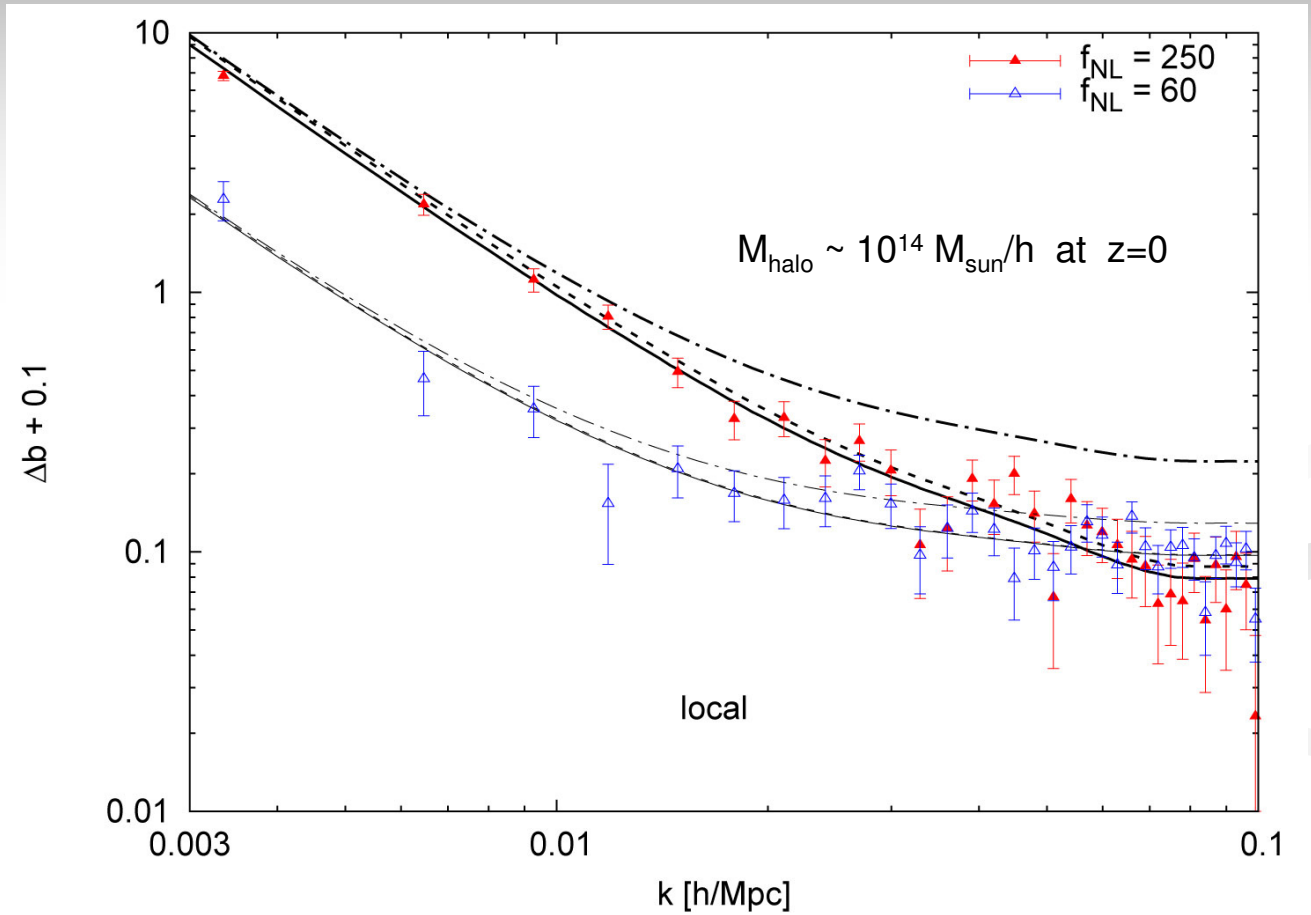

$$\Delta b(k) = \cancel{\Delta b_I} + f_{\rm NL}\left[b_1^G + \cancel{\Delta b_I} - 1\right]\frac{q\delta_c}{D(z)}\frac{\mathcal{F}_M(k)}{\mathcal{M}_M(k)}$$

NG halo bias – "orthogonal" ~ k^{-2}

(squeezed limit)

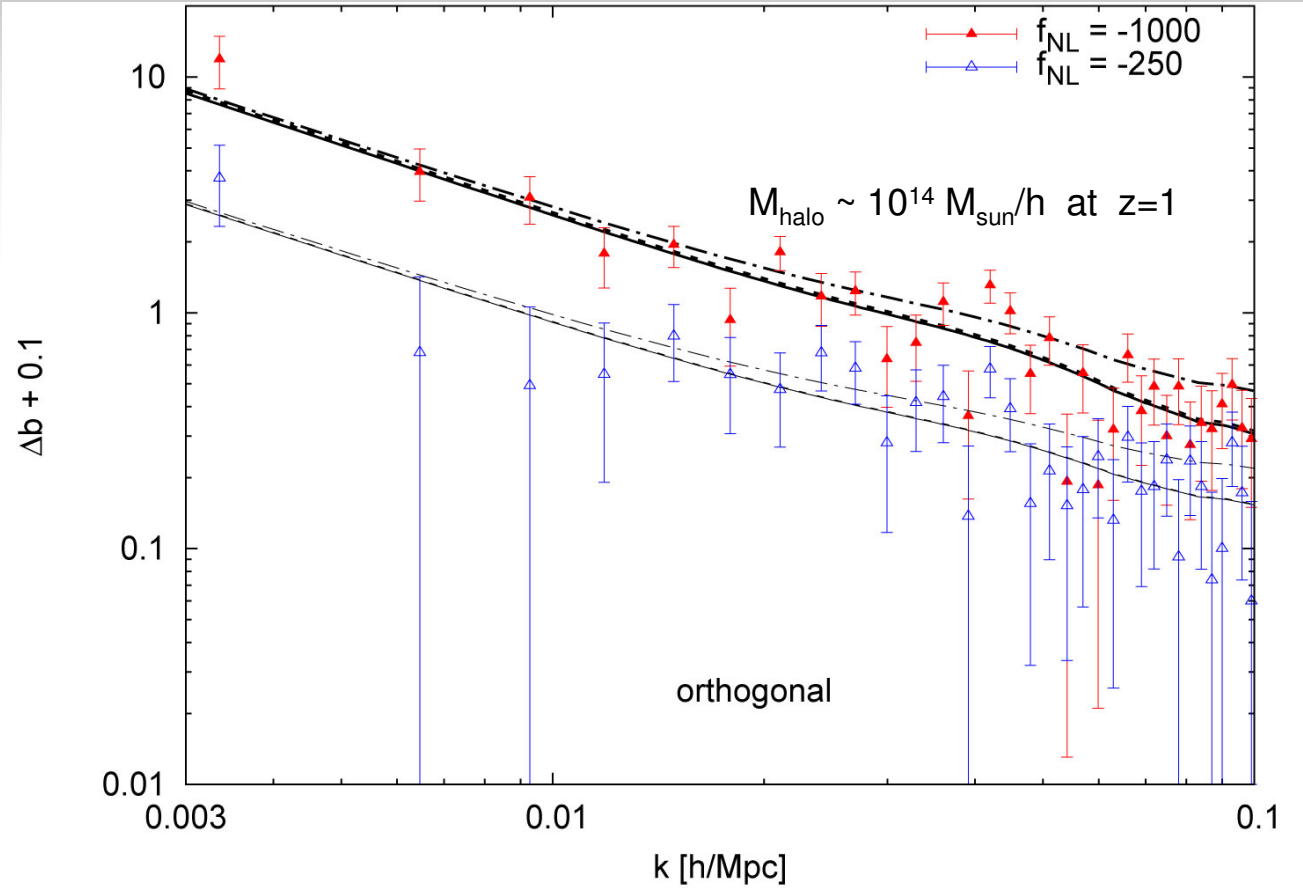

$$\Delta b(k) = \Delta b_I + f_{\rm NL}\left[b_1^G + \Delta b_I - 1\right]\frac{q\delta_c}{D(z)}\frac{\mathcal{F}_M(k)}{\mathcal{M}_M(k)}$$

NG halo bias – equilateral ~ k^{-1} (squeezed limit)

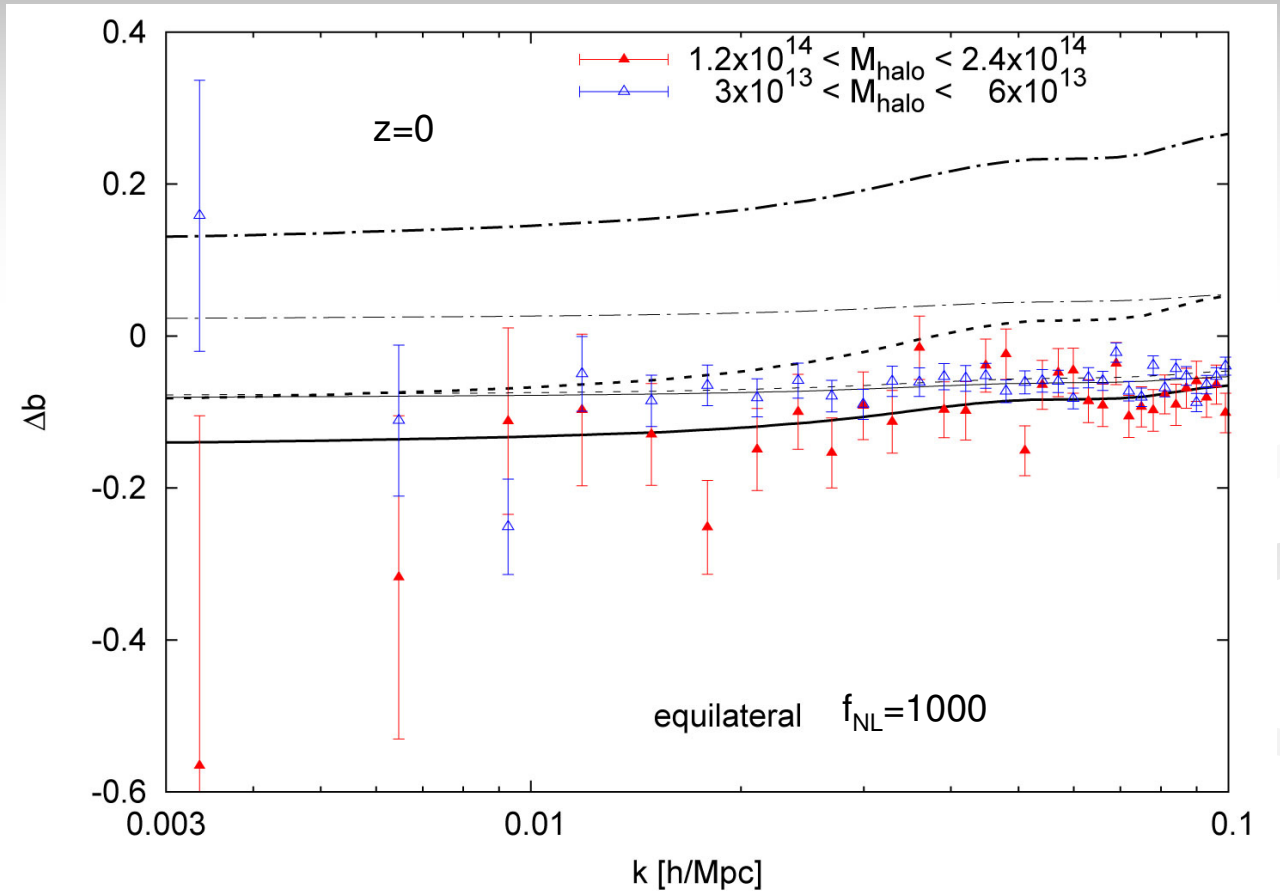

$$\Delta b(k) = \Delta b_I + f_{\rm NL}\left[b_1^G + \Delta b_I - 1\right]\frac{q\delta_c}{D(z)}\frac{\mathcal{F}_M(k)}{\mathcal{M}_M(k)}$$

Fitting results – local ~ k^{-3} (squeezed limit)

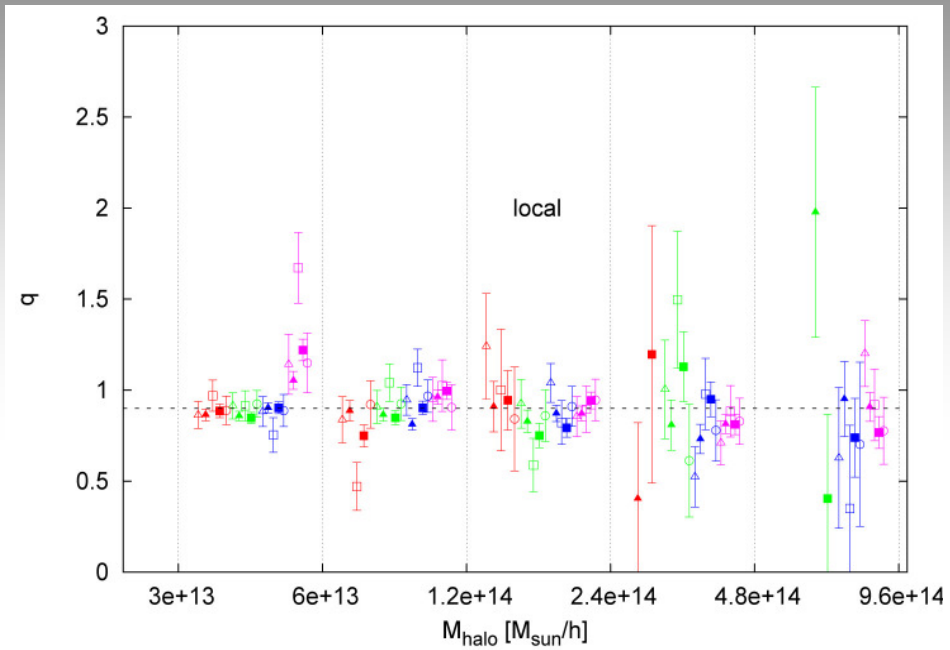

$$\Delta b(k) = \Delta b_I + f_{\rm NL}\left[b_1^G + \Delta b_I - 1\right]\frac{q\delta_c}{D(z)}\frac{\mathcal{F}_M(k)}{\mathcal{M}_M(k)}$$

For the local case, no significant mass or redshift dependence of the fudge factor q detectable

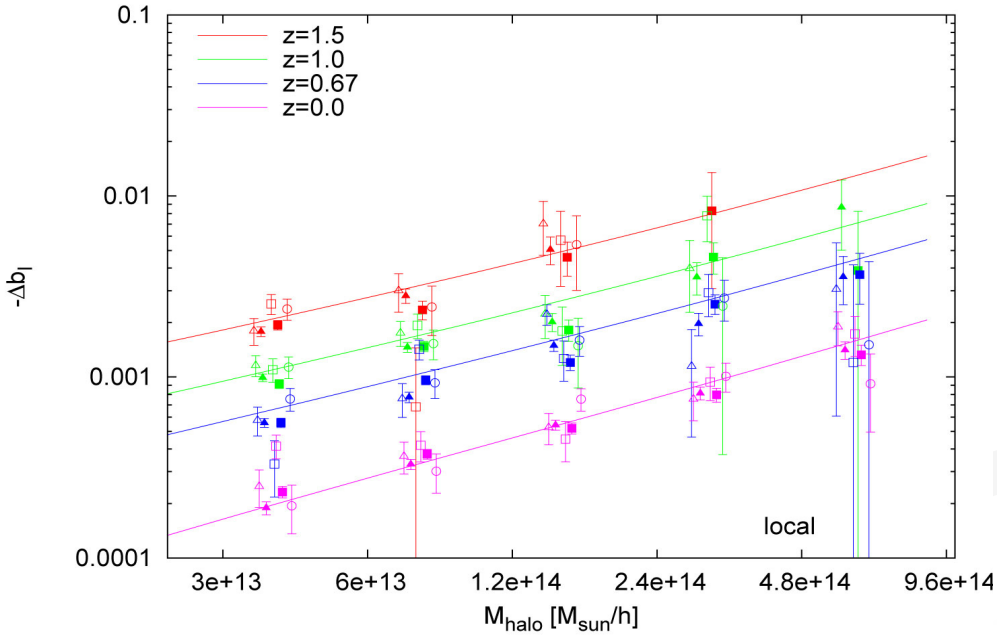

$$\Delta b_I = b_1^{NG} - b_1^G = -\frac{\partial \ln R^{NG}(M)}{\partial \delta_c}$$

Fitting results – "orthogonal" ~ k^{-2} (squeezed limit)

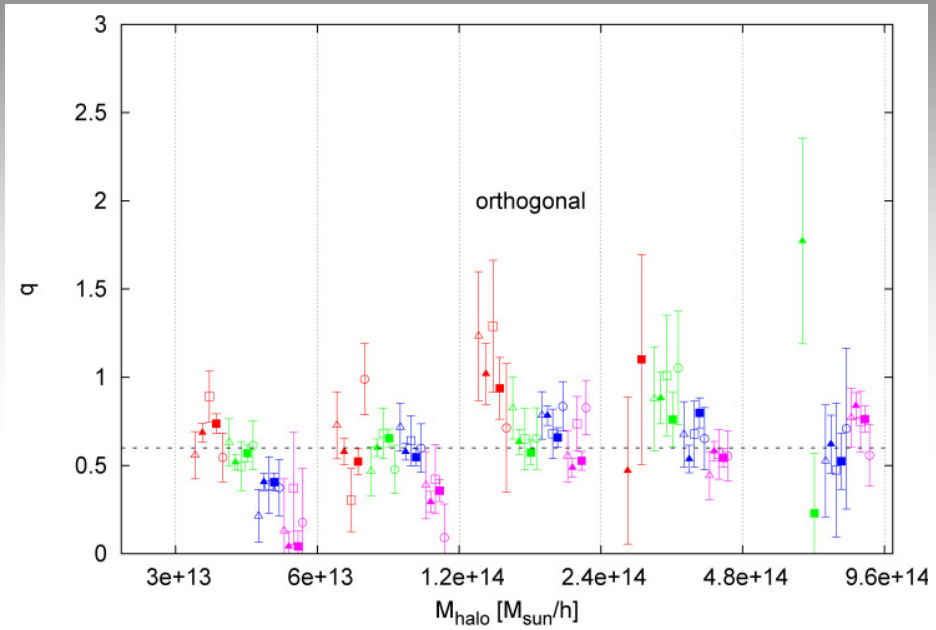

$$\Delta b(k) = \Delta b_I + f_{\rm NL}\left[b_1^G + \Delta b_I - 1\right]\frac{q\delta_c}{D(z)}\frac{\mathcal{F}_M(k)}{\mathcal{M}_M(k)}$$

low q: ~0.6-0.8

There are hints for a mass and redshift dependence of the fudge factor q!

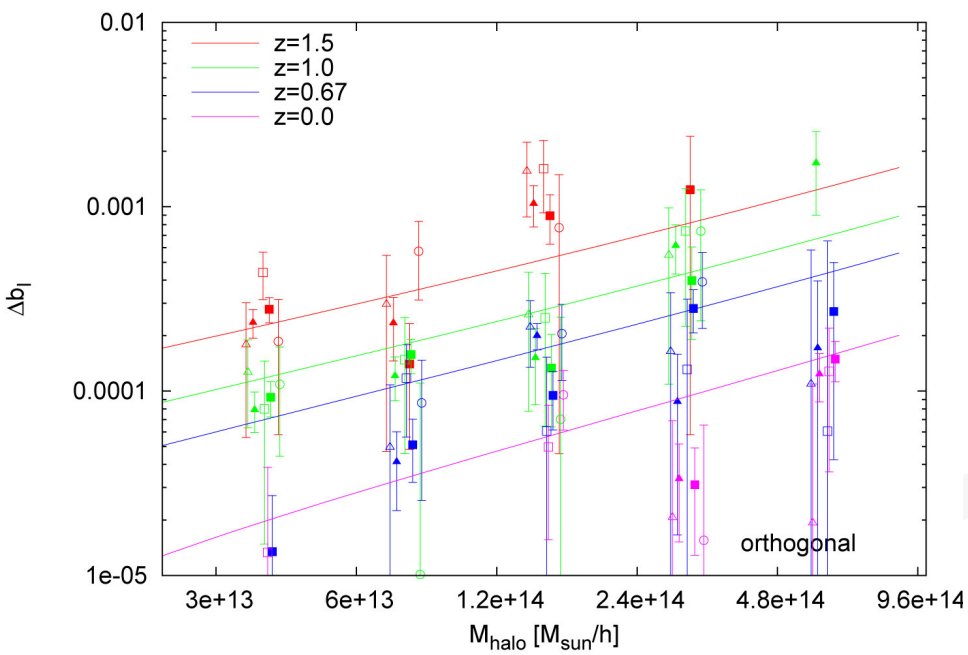

$$\Delta b_I = b_1^{NG} - b_1^G = -\frac{\partial \ln R^{NG}(M)}{\partial \delta_c}$$

Fitting results – equilateral ~ k^{-1} (squeezed limit)

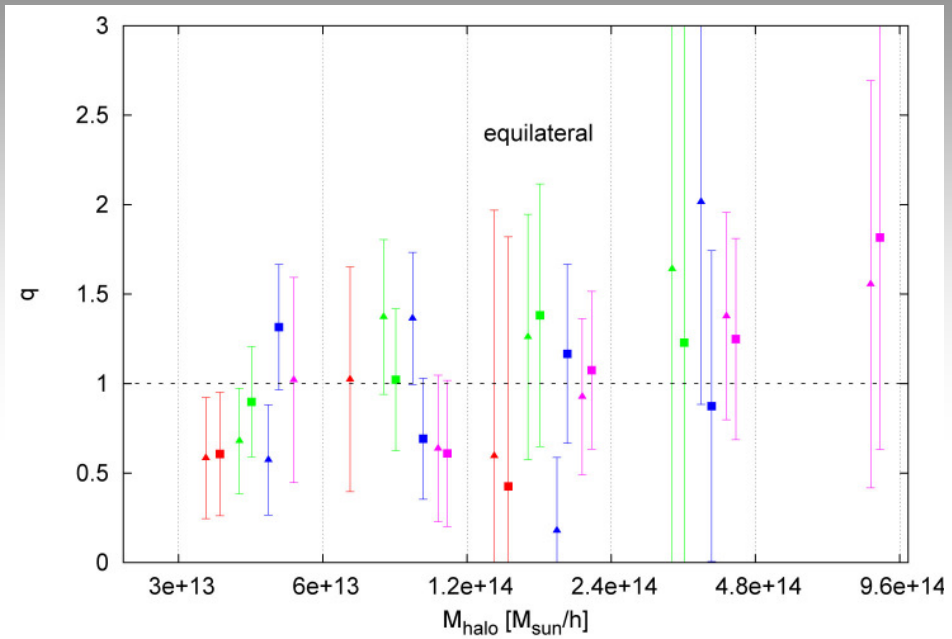

$$\Delta b(k) = \Delta b_I + f_{\rm NL}\left[b_1^G + \Delta b_I - 1\right]\frac{q\delta_c}{D(z)}\frac{\mathcal{F}_M(k)}{\mathcal{M}_M(k)}$$

Consistent with q=1, but very large error bars

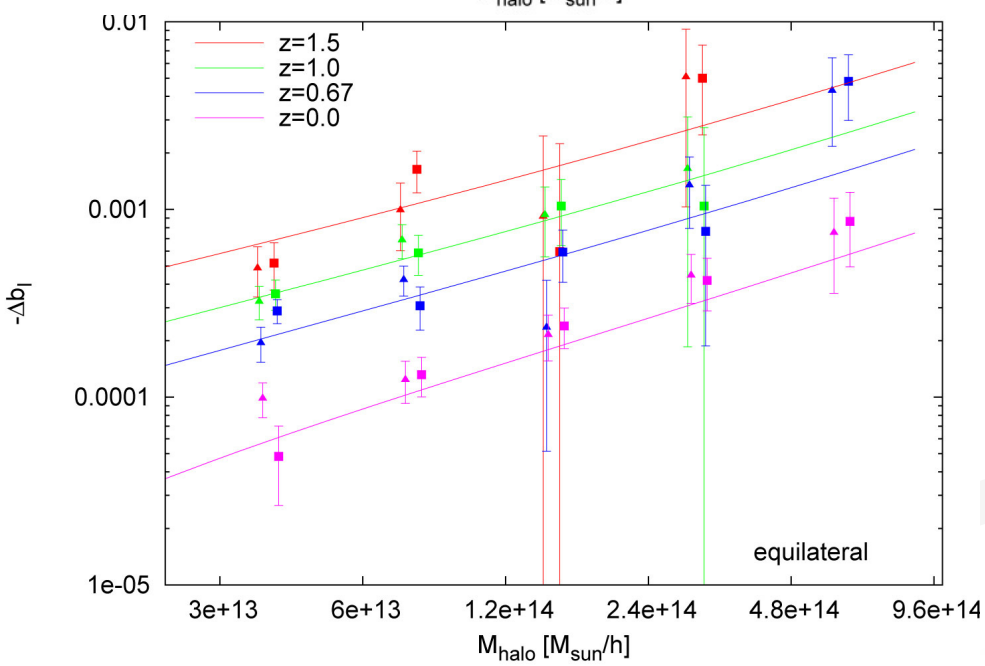

$$\Delta b_I = b_1^{NG} - b_1^G = -\frac{\partial \ln R^{NG}(M)}{\partial \delta_c}$$

Halo mass function

- Theoretical predictions for the ratio of mass functions

MVJ (Matarrese, Verde, Jimenez 2000)

$$R_{NG}(M,z,f_{NL}) = \exp\left[\delta_{ec}^3 \frac{S_{3,M}}{6\sigma_M^2}\right] \times \left|\frac{1}{6}\frac{\delta_{ec}}{\sqrt{1-\delta_{ec}S_{3,M}/3}}\frac{dS_{3,M}}{d\ln\sigma_M} + \frac{\delta_{ec}\sqrt{1-\delta_{ec}S_{3,M}/3}}{\delta_{ec}}\right|$$

LoVerde et al. 2008

$$R_{NG}(M,z,f_{NL}) = 1 + \frac{1}{6}\frac{\sigma_M^2}{\delta_{ec}} \times \left[S_{3,M}\left(\frac{\delta_{ec}^4}{\sigma_M^4} - 2\frac{\delta_{ec}^2}{\sigma_M^2} - 1\right) + \frac{dS_{3,M}}{d\ln\sigma_M}\left(\frac{\delta_{ec}^2}{\sigma_M^2} - 1\right)\right]$$

- The reduced skewness $S_{3,M}$ is the relevant parameter
- Also here a fudge factor is introduced $\boxed{\delta_c \longrightarrow \sqrt{q}\delta_c}$
- The value of q depends on the halo finder (Friends-of-friends or spherical overdensity)

Ratio of Mass function

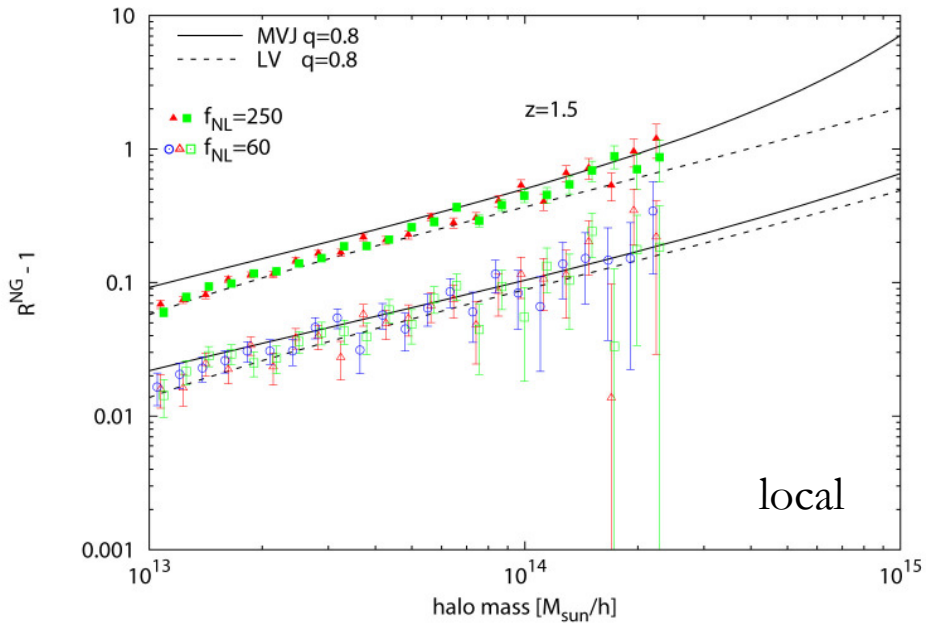

Theoretical predictions fit the data well, if a shape-dependent fudge factor is taken into account.

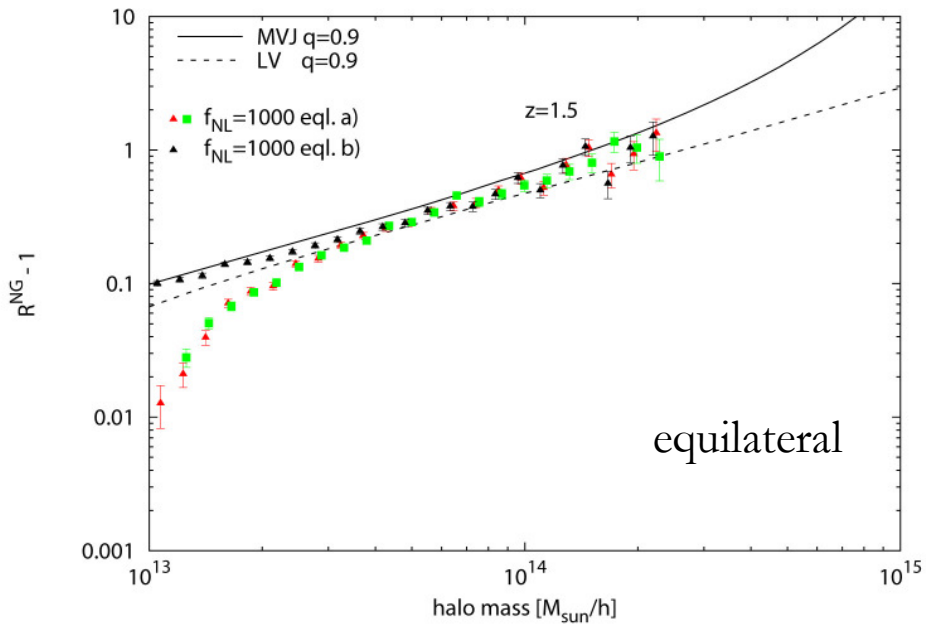

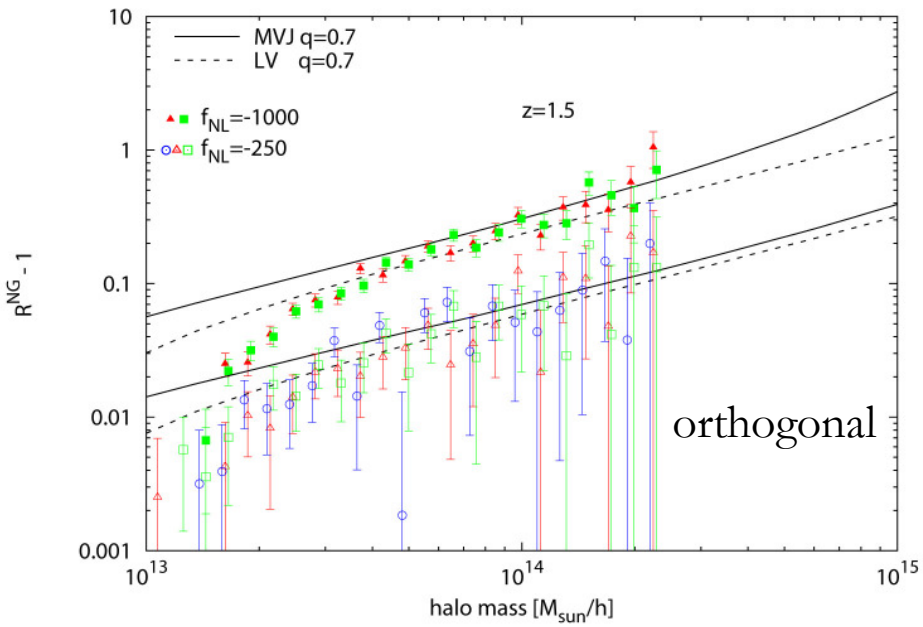

Conclusions

- Non-Gaussian initial condition for N-body simulations with generic bispectrum possible (but so far computationally expensive)
- N-body results for the (non)-local NG bias are consistent with theoretical predictions after the fudge factor q is calibrated
- This q-correction is shape-dependent and for some shapes q is redshift and mass dependent => **further modeling needed!**
- Interestingly, the fudge factors for the mass function and the halo bias predictions are consistent with each other. Probably more than a coincidence …
- **Advice:** Halo bias predictions need to be computed from the physical models not from templates

Bispectrum for different shapes

$$B(k_1, k_2, k_3) = 2 f_{\rm NL}^{\rm local} F^{\rm local}(k_1, k_2, k_3)$$

$$B(k_1, k_2, k_3) = 6 f_{\rm NL}^{\rm eql} \left(-F^{\rm local} - 2F^A + F^B\right)$$

$$B(k_1, k_2, k_3) = 6 f_{\rm NL}^{\rm enfl} \left(F^{\rm local} + 3F^A - F^B\right)$$

$$B(k_1, k_2, k_3) = 6 f_{\rm NL}^{\rm orth} \left(-3F^{\rm local} - 8F^A + 3F^B\right)$$

$$F^{\rm local}(k_1, k_2, k_3) = P(k_1)P(k_2) + P(k_2)P(k_3) + P(k_1)P(k_3)$$

$$F^A(k_1, k_2, k_3) = [P(k_1)P(k_2)P(k_3)]^{2/3}$$

$$F^B(k_1, k_2, k_3) = \left\{[P(k_1)]^{1/3}[P(k_2)]^{2/3}P(k_3) + 5{\rm cyc.}\right\}$$

Numerical Test I: Halo bias

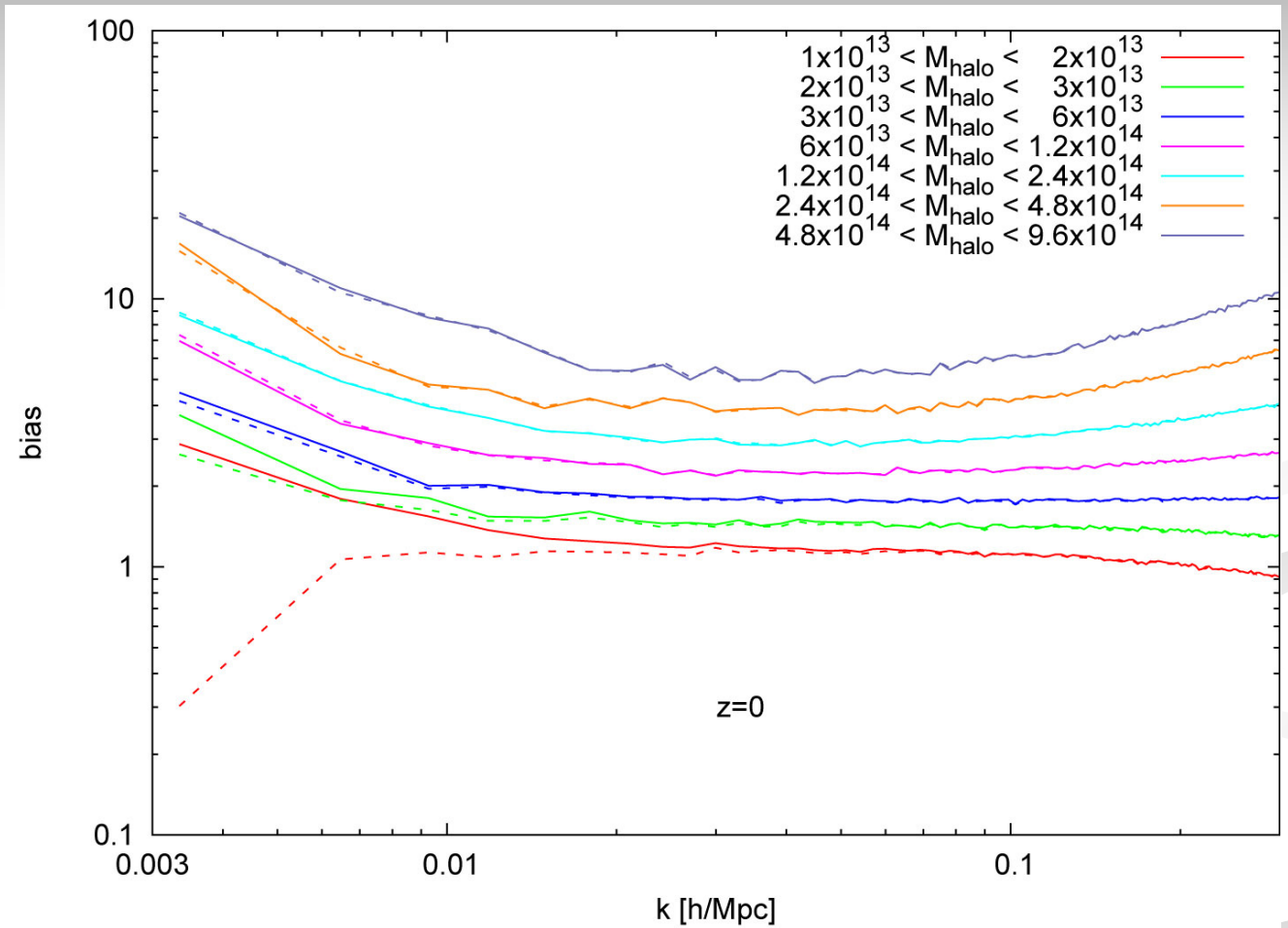

dashed lines: truncated non-Gaussian grid
solid lines: full non-Gaussian grid

Numerical Test II: Halo Mass Function

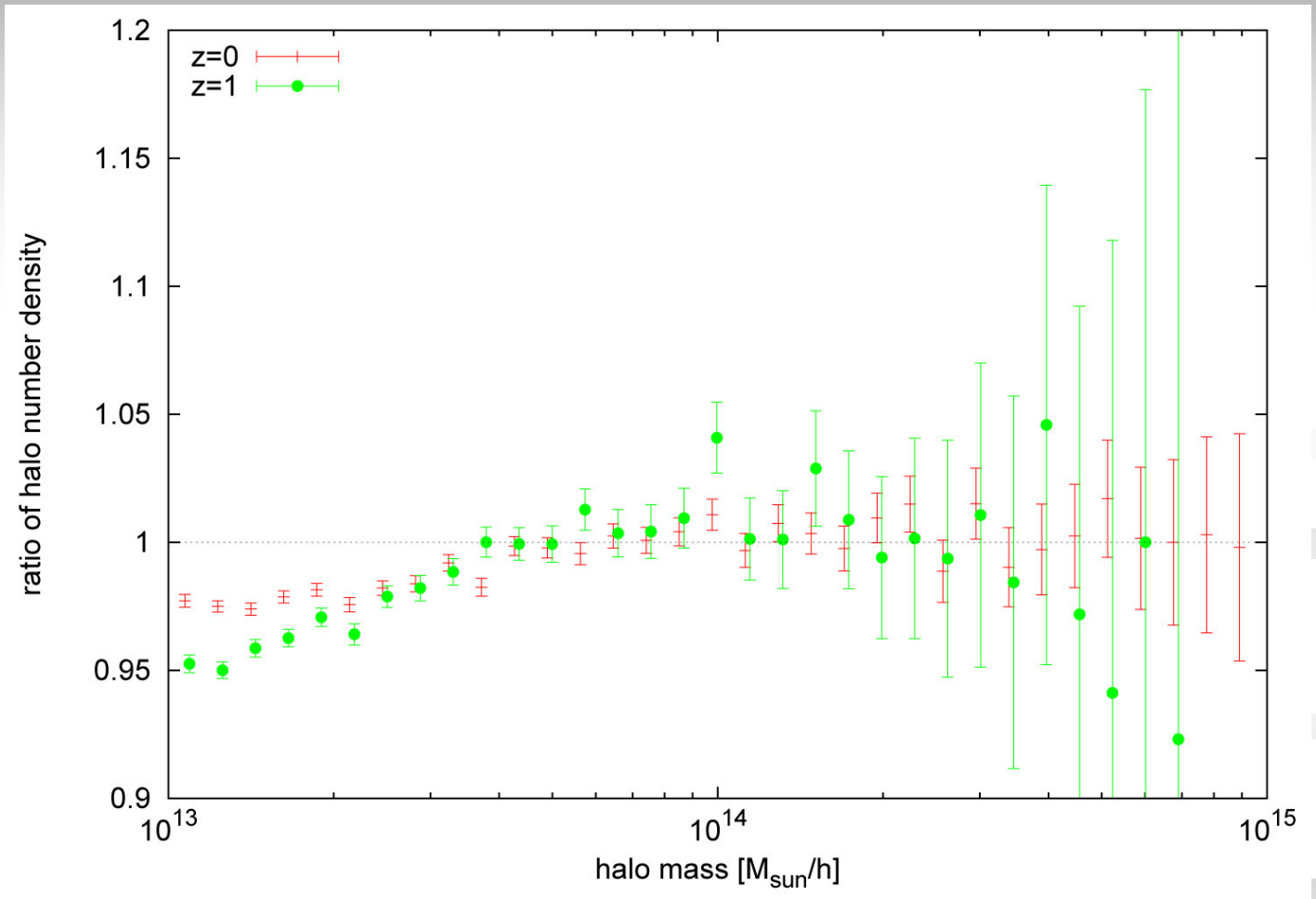

Truncated non-Gaussian grid vs. full non-Gaussian grid

Problem

- Second-order contributions of our old ansatz

$$\langle \Phi_{\mathbf{k}}^{NG} \Phi_{\mathbf{q}}^{NG} \rangle = \frac{1}{18} \delta^D(\mathbf{k}+\mathbf{q}) \int d^3k' \frac{B^2(k,k',|\mathbf{k}+\mathbf{k}'|)}{P(k')P(|\mathbf{k}+\mathbf{k}'|)}$$

  scales as $\mathbf{f_{NL}^2/k}$ for the enfolded and orthogonal template

- The NG halos bias scales as $\mathbf{f_{NL}/k}$ for the enfolded and orthogonal template

=> Effect is swamped by artificial power on large scales